EVS24
Stavanger, Norway, May 13-16, 2009

Simulation of the PEM fuel cell hybrid power train of an automated guided vehicle and comparison with experimental results

J.C.N. Bosma[1], P.A.Veenhuizen[2]
[1] *(corresponding author) HAN University, P.O. Box 2217, 6802 CE Arnhem, the Netherlands, hans.bosma@han.nl*
[2] *HAN University, P.O. Box 2217, 6802 CE Arnhem, the Netherlands, bram.veenhuizen@han.nl*

Abstract

At HAN University research has been started into the development of a PEM fuel cell hybrid power train to be used in an automated guided vehicle. For this purpose a test facility is used with the possibility to test all important functional aspects of a PEM fuel cell hybrid power train. In this paper the first experimental results of the testing of the power train are presented, driving a drive cycle designed especially for this automated guided vehicle. Experimental results are compared to results for this specific drive cycle from the simulation of the power train with the QSS-toolbox, using a simple battery model of our specific energy storage situation. Further some recommendations for improvement of the test facility are given, resulting from restrictions encountered during the experiments.

Keywords: simulation, modelling, HEV (hybrid electric vehicle), fuel cell, nickel cadmium battery

1 Introduction

HAN University is developing a power train of an automated guided vehicle (AGV). This AGV is designed to transport passengers in the open air under high temperature conditions. It should be able to operate uninterruptedly for 18 hours, covering over 300 kilometres. This is not possible to do with batteries as the only power source because of the required energy amount. Therefore the use of a PEM fuel cell as a range extender is considered.

This paper describes the research into the development of a PEM fuel cell hybrid power train. Special attention is paid to the simulation of the power train with the QSS-Toolbox and comparison with experimental results from the test model of the AGV in the laboratory of HAN University in Arnhem (NL).

2 AGV power train simulation

2.1 AGV drive cycle

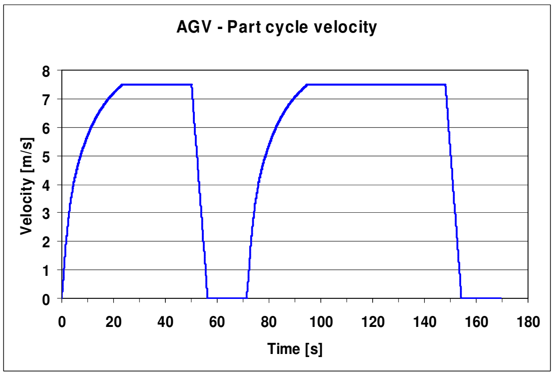

Figure 1: Part cycle, velocity

The maximum required velocity of the AGV is 7.5 m/s. The maximum acceleration of the vehicle, determined by the torque-speed curve of the

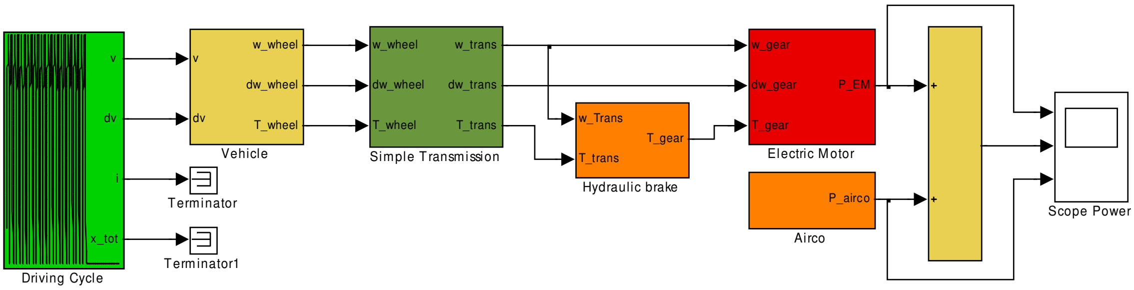

Figure 2: QSS-model to evaluate the total power demand of the AGV

electric motor in the AGV, is approximately 1.2 m/s^2. The mean deceleration of the vehicle is 1.2 m/s^2, due to the use of a hydraulic braking system. The total drive cycle of the AGV consists of 12 part cycles as shown in Fig. 1, followed by 240 s. of stand still. Thus the total cycle time is 2268 s.

This total drive cycle has to be repeated uninterruptedly until the total time of 18 hours is completed.

2.2 AGV power demand

The main power to be supplied by the power supply of the AGV is required to drive the cycle as shown in Fig. 1. Further, since the AGV will be operating under high temperature conditions, it will be equipped with an air conditioner. The power demand of this air conditioner will switch from 0.7 kW (low) to 1.3 kW (high) in a 50% duty cycle. The total power demand for driving and cooling the AGV is evaluated with the QSS-model in Matlab/Simulink [1] as shown in Fig 2. From left to right this model consists of the following subsystems:

- drive cycle
- vehicle
- gear box
- hydraulic brake
- electric motor / generator
- air conditioner

In the subsystem Vehicle wheel speed and wheel torque are calculated, which are required to overcome frictional, aerodynamical and inertial forces while driving the drive cycle. As a result the required power at the wheels is calculated as shown in Fig. 3. This figure shows that the maximum required power at the wheels is approximately 7.5 kW. When the AGV is decelerating a maximum power of almost 20 kW is made available.

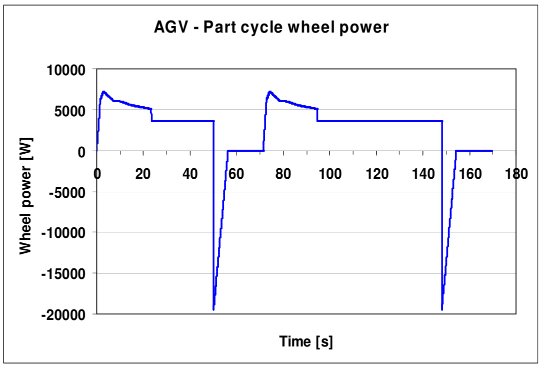

Figure 3: Part cycle, power at the wheels

All the subsystems at the right hand side of the Vehicle block introduce power losses, eventually resulting in a much higher power required from the energy supply. The function of the gear box is to adjust wheel speed and torque to the speed and torque from the electric motor. In this situation a simple transmission with a fixed gear ratio is sufficient.

The calculated speed and torque of the electric motor are used as steering signals for the hardware model of the AGV in the laboratory of HAN University.

During deceleration the electric motor is working as a generator. A hydraulic brake is applied in the AGV to obtain the required deceleration of 1.2 m/s^2, even when the braking power is higher than the power that can be regenerated by the motor/generator.

The total power demand of the AGV is shown in Fig. 4. This power has to be supplied by the PEM fuel cell in combination with a battery. The maximum power demand is approximately 12 kW. The maximum amount of regenerated power is over 5 kW.

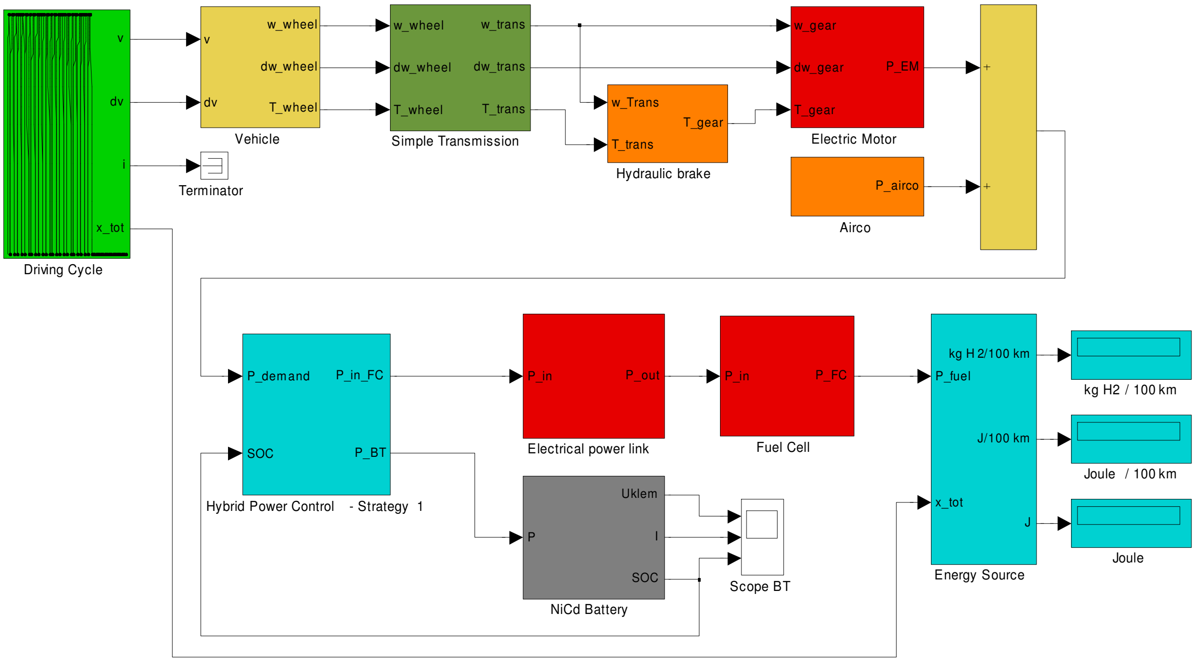

Figure 5: QSS-model of the AGV, including the power supply

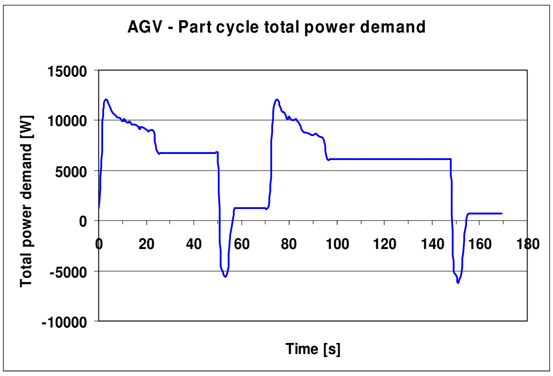

Figure 4: Part cycle, total power demand

2.3 Modelling of power supply

The QSS-model of the complete AGV is shown in Fig. 5. In this figure the set-up of Fig. 2 is extended with a hybrid power supply, consisting of a fuel cell system, a battery and a power control unit. The power to drive the AGV and to operate the A/C unit is provided either by the battery and the fuel cell individually or by a combination of these two. The energy flows are controlled by a hybrid power controller. This controller can be designed in several ways. One option is to use the fuel cell system as an on-board charger to maintain the battery's state of charge within a restricted band, irrespective of the actual power demand. Another option is to operate the fuel cell system in a fixed (or slowly varying) working point, using the battery to meet the fast variations in the power demand pattern. It is the aim of the model to be able to evaluate various hybrid power controller models and to compare results with experiments.
Since the fuel cell hybrid power train test facility at HAN University [2] does not have the possibility to regenerate the braking power, regenerative braking is ignored in simulation also. Furthermore in this stage of the research also the power demand of the A/C unit is not taken into account.

2.3.1 Battery model

In the simulation a simple battery model is used, describing the battery as an ideal voltage source in series with an internal resistance R_2 and the combination of a resistance R_1 and a capacitance C in series. The model is shown in Fig. 6.

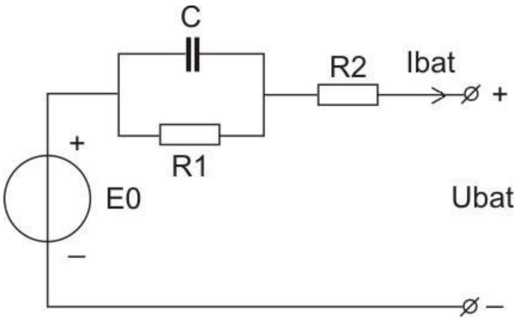

Figure 6: Simple battery model as used in the simulation

It is used in the simulation model to calculate the voltage and the current of the battery and its State of Charge (SoC), using the power demand as input. This battery model replaces the battery model, which is standard available within the QSS-toolbox.

For the 180 Ah NiCad battery used in the experiments the values of C, R_1 and R_2 have been determined experimentally from the time dependent behaviour of the battery, resulting in $R_2 = 29\ m\Omega$, $R_1 = 16\ m\Omega$ and $C = 25000$ F.

This model requires the relation between the voltage E_0 of the ideal voltage source and the State of Charge of the battery. This relation has been determined experimentally and is shown in Fig. 7.

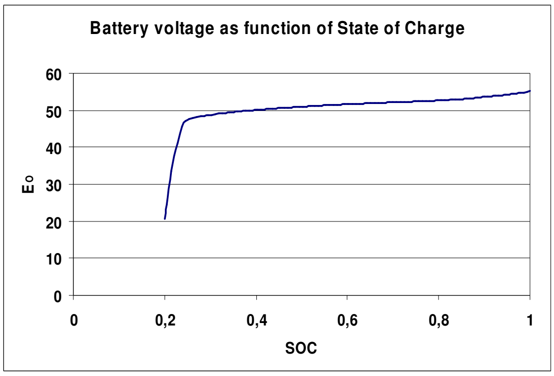

Figure 7: Battery voltage as function of SoC

The battery model has been tested by simulating a run with the AGV drive cycle, neglecting the power demand from the A/C unit and the power input from the fuel cell system. In this situation the electric motor is powered only by the battery. The results of this simulation will be compared to experimental data.

2.3.2 Fuel cell model

The PEM fuel cell model as used in the QSS-model is based upon the polarisation curve of a single fuel cell. From the fuel cell's power demand the required hydrogen input power of the fuel cell is calculated, taking into account heat losses of the fuel cell, idle power, air compressor and other auxiliary power requirement. The fuel cell stack used in our experiments and in the simulations is a 120 cell PEM fuel cell stack from Nedstack, with an effective fuel cell area of $0.02\ m^2$.

2.3.3 Hybrid power controller model

In this paper a simple hybrid power controller is used, setting the fuel cell system to a fixed output power and allowing the battery to meet the variations in the power demand pattern. As is shown in Fig. 4, the power demand is varying very strongly with time; this makes high demands upon the simple battery model used in the simulation.

3 Battery model evaluation

In Fig. 8 a comparison is made between the simulated battery voltage and the measured battery voltage over the total drive cycle of the AGV, in the situation without power demand from the A/C unit and power input from the fuel cell. The minima in each plot represent the battery voltage at maximum power to the electric motor, i.e. while accelerating the AGV. The maxima in each plot occur when the AGV is decelerating or stands still; in this situation no electric power is needed. The constant levels of the battery voltage in each plot (somewhere halfway between minima and maxima) represent the situations in which the AGV is driving at maximum velocity. Fig. 8 shows that the resemblance between the measured and simulated battery voltage is quite good. The drop of the battery voltage over the total cycle is approximately equal for the simulated results and the measurement.

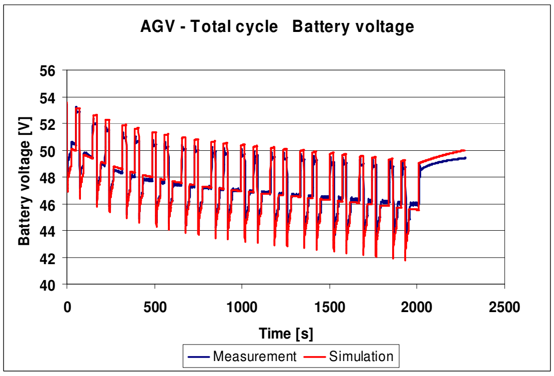

Figure 8: Total cycle, measured and simulated battery voltage

This resemblance can also be illustrated by Fig. 9, showing just a part of the total drive cycle (cf. Fig. 1). The maximum power phase (at approximately 175 sec. and 245 sec.), the decelerating/standstill phase (220-240 sec. and 320-330 sec.) and the maximum velocity phase (195-220 sec. and 265-320 sec.) can clearly be recognized. The small rise in the battery voltage during the deceleration phase is caused by the inertia of electric motor, working as a generator.

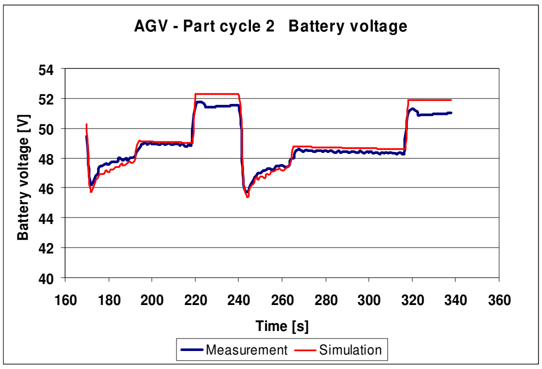

Figure 9: Part cycle 2, measured and simulated battery voltage

4 Evaluation of power supply including PEM fuel cell

Experiments have been performed to investigate the power train behaviour in the situation that the PEM fuel cell is used to charge the battery during execution of the drive cycle. In this situation there is a power flow from the battery to the electric motor (discharge), comparable to the situation described in section 3, and a power flow from the fuel cell system to the battery (charge). The measured power flows connected to charging the battery are shown in Fig. 10. In this figure three power flows are presented, P_{stack} being the power produced by the fuel cell system, P_{charge} being the power fed tot the battery and P_{loss} being the difference between P_{stack} and P_{charge}, representing the power loss in the DC/DC converter [2].

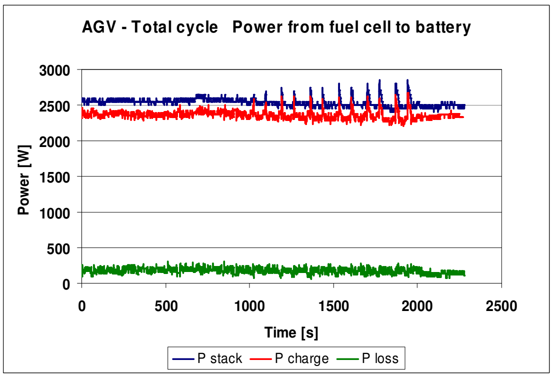

Figure 10: Total cycle, measured power flows from fuel cell to battery

The power to charge the battery P_{charge} is rather constant over the first half of the total cycle. In the second half of the cycle peaks occur in the power signal, which are correlated to the maximum power demand phases in the drive cycle. In the second half of the cycle the battery voltage drops below the voltage of the fuel cell system, firstly only during the moments of maximum power demand, but later on in the cycle most of the time. This is shown in Fig. 11. Since the DC/DC converter is working according to the step up principle, in this situation the converter does not work as a converter anymore and basically then the battery is connected directly to the fuel cell system, resulting in a higher value of P_{charge}.

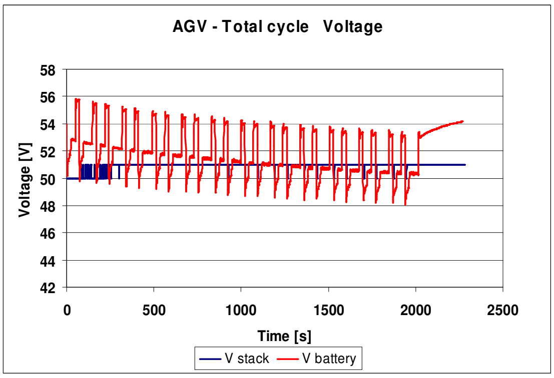

Figure 11: Total cycle, measured voltage of battery and fuel cell stack

To assure a proper working of the DC/DC converter the fuel cell system should be operated at a lower voltage level, resulting in a higher output current assuming a constant output power. An other option is to replace the DC/DC converter by a converter of the step up / step down type.

Comparing Fig. 11 to Fig. 8 shows that due to charging the battery while running the drive cycle, the voltage drop of the battery is less than in the situation without charging and the variation of the battery voltage over a part cycle is less (no charging: ≈ 7 V; charging: ≈ 5 V), as one would expect.

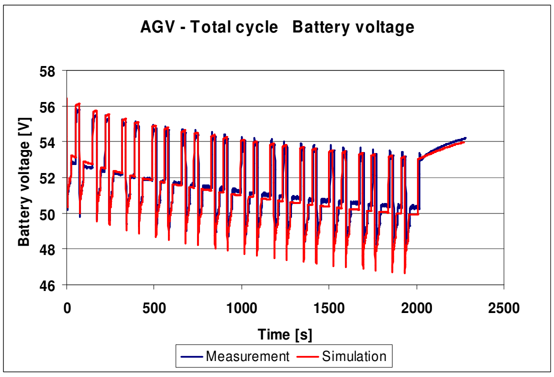

Figure 12: Total cycle, measured and simulated battery voltage

Also in the situation of charging the battery with a fixed fuel cell power, the resemblance between the measured and the simulated battery voltage is quite good and comparable with the results without charging, as is shown in Fig. 12.

This is also illustrated in Fig. 13, showing the battery voltage in only the first part cycle. As in Fig. 9 the various phases of the drive cycle can easily be recognized.

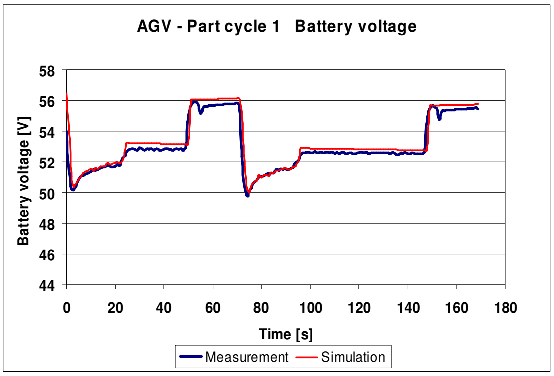

Figure 13: Part cycle 1, measured and simulated battery voltage

The measured net power from the battery is shown in Fig. 14. The net power is the resulting power from the discharging power (power from the battery to the electric motor) and the charging power (power from fuel cell system to battery). Net power is positive when discharging and negative when charging.

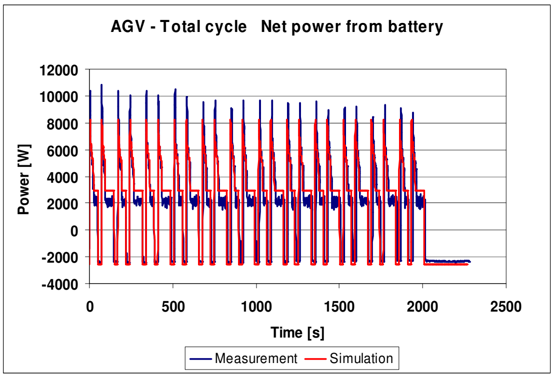

Figure 14: Total cycle, net power flow from battery

The overall resemblance of the measured and the simulated net power is quite good. However, the difference in net power when driving at maximum speed (approximately at 2000 W) needs further investigation.

Furthermore from Fig. 11 it is clear that in this measurement the power input from the fuel cell system is too low to compensate the power output to the electric motor; as a result the State of Charge of the battery will drop. However, when the fuel cell system is operated at a sufficiently high power output level in combination with the desired drive cycle, the temperature of the air compressor of the fuel cell stack becomes too high; the fuel cell system will then shut down automatically.

These experimental problems made it impossible to do experiments with the AGV drive cycle, described in section 2, with at the same time a properly working DC/DC converter and the battery having an equal State of Charge at the end of the cycle as at the start. A comparison of energy consumption between experiment and simulation therefore is not possible.

It is recommended to adjust the hardware of the test facility to be able to perform experiments in the way described above.

References

[1] L. Guzzella et. al., *Vehicle Propulsion Systems*, ISBN 3-540-25195-2, Springer, 2005

[2] B. Veenhuizen et al., *Fuel cell hybrid drive train test facility*, EVS24, Stavanger, 2009

Authors

J.C.N. (Hans) Bosma, Dr., HAN University, Arnhem, the Netherlands.

Dr. J.C.N. Bosma received his M.Sc. degree in technical physics form the Technical University of Eindhoven, The Netherlands in 1981. In 1987 he received his PhD degree from the Technical University of Eindhoven on the subject of gasdynamic aspects of linear MHD-generators.

In 1987 he joined Gastec NV, Apeldoorn, The Netherlands, were he did research on combustion processes in domestic and industrial gas appliances. From 1996 to 2004 he was manager of the departments Industrial gas appliances and Domestic gas appliances respectively. In 2004 he joined HAN University as a member of the vehicle mechatronics research group

P.A. (Bram) Veenhuizen, Dr., HAN University, Arnhem, the Netherlands.
Dr. P.A. Veenhuizen received his M.Sc. degree in experimental physics from the Free University of Amsterdam, The Netherlands in 1984. In 1988 he received his PhD degree from the University of Amsterdam on the subject of Electronic properties of Ce- and U-based compounds. In 1988 he joined SKF Engineering and Research Centre where his work focused on electromagnetic detection techniques for material characterization and X-ray characterization of material fatigue. In 1995 he joined van Doorne's Transmisie bv, where he was responsible for the realization of some advanced drive train projects. In 2002 he was appointed assistant professor in the CST group of the ME department of the Eindhoven University of Technology. Since 2005 he is also professor in vehicle mechatronics at the HAN University in Arnhem..